ACS APPLIED MATERIALS & INTERFACES

Research Article

www.acsami.org

Biofunctionalization of 3D Nylon 6,6 Scaffolds Using a Two-Step Surface Modification

Edin Nuhiji,[‡,†] Cynthia S. Wong,[‡,†] Alessandra Sutti,[‡] Tong Lin,[‡] Mark Kirkland,[‡] and Xungai Wang*[,‡,§]

[‡]Institute for Frontier Materials, Deakin University, Geelong, Victoria, Australia, 3217

[§]School of Textile Science and Engineering, Wuhan Textile University, Wuhan, China

ABSTRACT: Nylon is a relatively inert polymer. The ability to easily functionalize nylon with biomolecules will improve the utilization of nylon in biological systems. A potential use of the biofunctionalized nylon scaffolds is in devices for cell therapeutics that can specifically select cells present in small numbers, such as hematopoietic stem cells. This study developed a versatile and simple two-step technique combining oxygen plasma treatment with wet silanization to graft biomolecules onto nylon 6,6 3D porous scaffolds. Scaffolds that were exposed to oxygen plasma exhibited up to 13-fold increase in silane attachment ((3-mercaptopropyl)trimethoxysilane/(3-aminopropyl)trimethoxysilane) compared to untreated scaffolds. To address the limitation of nondestructive characterization of the surface chemistry of 3D scaffolds, fluorescent CdSe/ZnS nanoparticles were used as a reporting tool for $-NH_2$ functionalized surfaces. Scaffolds that were covalently bound with neutravidin protein remained stable in phosphate buffered saline up to four months. Functionality of the neutravidin-grafted scaffolds was demonstrated by the specific binding of CD4 cells to the scaffold via CD4-specific antibody. Ultimately, these neutravidin-functionalized 3D nylon scaffolds could be easily customized on demand utilizing a plethora of biotinylated biomolecules (antibodies, enzymes and proteins) to select for specific cell of interest. This technique can be extended to other applications, including the enhancement of cell-scaffold interactions.

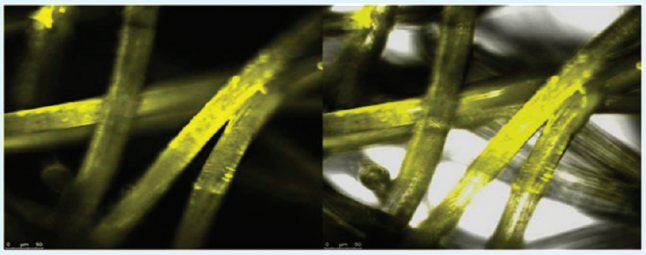

KEYWORDS: *biofunctionalization, 3D porous scaffolds, surface modification, silanes, vacuum plasma treatment, nylon*

1. INTRODUCTION

Polymeric materials are a versatile tool utilized in biomaterials research and development approaches, particularly for medical applications. The main advantage of using polymeric materials is the ability to tune their physical properties to suit a bio-application on demand. Three-dimensional (3D) polymeric scaffolds have shown great promise as the next generation of scaffold architecture.[1,2] The ability of these 3D scaffolds to offer increased surface area combined with novel geometrics such as interconnected pores and networked channels present them as ideal candidates for structural support for tissue regeneration[3,4] and reconstructive orthopedic surgery.[5,6]

Regenerative medicine is not the only area that utilizes 3D polymeric scaffolds. Increasingly, in the field of stem cell therapeutics, 3D polymeric scaffolds are being used in vitro to culture and expand stem cells such as hematopoietic stem cells, which can be used to treat leukemia.[7,8] However, hematopoietic stem cells are present in vivo in minute amounts such that without isolation and expansion in vitro, treatment via these cells will be rendered inefficient or lead to limited success.[9,10]

Therefore, there is a need to functionalize polymeric scaffolds so that they provide an environment whereby cells can be specifically selected in vitro. The present study has chosen to use nylon as the scaffold's base polymer. This is because nylon is one of the most widely used polymers across diverse industries, ranging from automotive to food. Manufactured nylon products include clothing, parachutes, mechanical parts and food packaging, and in the biomedical field it is commonly utilized for suture production. The thermomechanical properties, excellent accessibility, and low cost make nylon an excellent candidate for 3D scaffold and biomaterials development strategies. A major drawback of native nylon is its relatively inert surface properties, which limits the possibility to chemically bind biomolecules directly onto the surface of native nylon.[11−13]

Many scaffold surface modification strategies using chemical and biomolecular functionalization are available to further enhance biocompatibility and cell proliferation.[13−15] These methods are usually substrate-dependent, require multiple processes and are optimized on a case-by-case basis.[16−18] Of these approaches, because of nylon's chemical inertness, only a few have been tailored to modify nylon for the attachment of biomolecules. These methods are generally quite complex and involve multiple steps.[11,19−22] Therefore, a simpler approach is sought for the biofunctionalization of nylon surfaces.

Plasma-induced surface modification provides a platform to activate inert polymers, including nylon, by altering their surface chemistry.[23] Plasma treatment can be carried out in the

Received: January 17, 2012
Accepted: May 17, 2012
Published: June 4, 2012

presence of gases such as Ar, N_2 and O_2 (gas plasma) or in the presence of functional monomers which are grafted directly onto the material surface during the treatment (plasma polymerization).[24] Plasma polymerization can be performed with a limited range of molecules, often requiring further modification steps to functionalize surfaces with biomolecules. Oxygen plasma treatment, on the other hand, is widely used to introduce a variety of polar functional oxygen species on a material surface (e.g., hydroxyl, carboxyl and peroxides).[25−27] However, the effects of oxygen plasma on surface energy and chemistry are transient. Hence, plasma treatments typically need to be accompanied by a bioconjugation step whereby a linker and a biomolecule are grafted on the treated surface. Alkoxysilanes constitute the ideal linker for surfaces that carry active −OH groups:[28,29] the silane binds to a hydroxylated surface via a hydrolytic/condensation reaction involving the three available alkoxy groups (Figure 1).

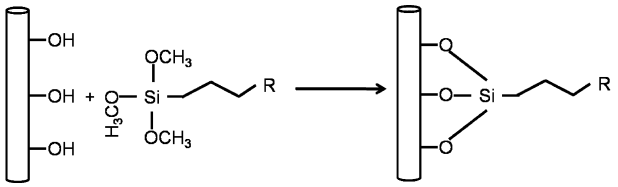

Figure 1. Chemical reaction of APS (R = NH_2) or MPS (R = SH) with a hydroxylated surface.

The methods developed for the direct deposition of silanes to nylon may require the deposition of sol−gel-SiO_2 primer layers,[11,19,30] or may vary depending on the silane used.[16] TriStar Plastics Corp USA demonstrated a more generic and gas-phase-only approach to modify polymer surfaces using organosilanes.[31] Although more universal, this technique still involved multiple steps, along with the need for accurate management of hazardous gaseous organosilanes. These shortcomings can be addressed via the use of wet-chemical silanization methods which present several advantages including ease of application to porous and nanomaterials. Nonetheless, the limited reactivity of native nylon toward alkoxysilanes remains an issue. Coupling the ability of oxygen plasma treatment to increase the number of reactive species onto the polymeric surface with the advantages of wet silanization may provide a means of overcoming the aforementioned disadvantages. Although a plethora of alkoxysilanes is available and the two techniques are individually well-established, to the best of the authors' knowledge, the combination of oxygen-plasma and alkoxysilanes applied to non-siloxane-based polymeric scaffolds have not been investigated.

This present study proposes a versatile two-step combination of plasma treatment and wet silanization to enable the grafting of biomolecules on nylon 6,6 surfaces via established bioconjugation techniques. Nylon 6,6 was used in this study to demonstrate the ability of the developed technique to functionalize relatively inert polymers with biomolecules. Two alkoxysilanes, (3-aminopropyl)trimethoxy silane (APS) and (3-mercaptopropyl)trimethoxy silane (MPS), were chosen as linkers to demonstrate the availability of the thiol and amine groups for the bioconjugation process.[32,33] Specifically, this study aimed to:

(1) Develop a two-step surface modification involving plasma and silane chemistries for a 3D nylon 6,6 porous scaffold.
(2) Validate the presence of MPS (−SH) and APS ($-NH_2$) silane on the modified scaffold.
(3) Assess the ability to functionalize the silane-modified scaffold with biomolecules.

2. EXPERIMENTAL SECTION

Materials. Nylon 6,6, 15 Denier staple fiber of 35 μm diameter was sourced from Solutia, USA. (3-Mercaptopropyl)trimethoxysilane (MPS, 95%), (3-aminopropyl)trimethoxysilane (APS, 95%), ammonium hydroxide (25 wt % NH_3 in water), analytical grade ethanol, and 2-propanol were acquired from Merck (Victoria, Australia). Sulfuric acid, cysteine hydrochloride monohydrate, phosphate buffered saline (PBS) powder (pH 7.4 reconstituted in deionized water), polyoxyethylene sorbitan monolaurate (Tween 20), and ethylenediaminetetraacetic acid (EDTA) were purchased from (Sigma Aldrich, Australia). Milli-Q grade (R > 18 M Ω cm) and deionized water was used throughout. CdSe/ZnS core−shell nanocrystals (NCs) were kindly provided by Dr Tich Lam Nguyen and Christian Potzner of the University of Melbourne. All cores-shells were synthesized and stabilized in aminopentenol using previously published methods.[34,35] CdSe/ZnS NCs of 5.9 nm in diameters utilized in the experiments described in this paper observed the emission maxima λ_{max} of 572 nm. A solution of 0.1 M sodium phosphate dibasic heptahydrate (Fluka, USA) buffer pH 8.0 was combined with 1 mM EDTA for the Ellman's reagent assay. Substrate Reagent Pack for ELISA was purchased from R&D Systems, USA and used as received. Maleimide-Activated NeutrAvidin Protein (mNtv), Ellman's Reagent, biotinylated horseradish peroxidase enzyme (biotin HRP), and Tris(2-carboxyethyl)-phosphine (TCEP) were purchased from Thermo Scientific Pierce (Rockford, USA) and used as prescribed by the manufacturer. Biotinylated mouse antihuman CD4 antibody and biotinylated IgG antibody were purchased from Sapphire Bioscience (Sydney, Australia). LIVE/DEAD Kits for Mammalian Cells was purchased from Life Technologies (Victoria, Australia).

Instrumentation. *a. Microscopy and X-ray Photoelectron Spectroscopy.* Fluorescent images were captured using a confocal microscope system (Leica TCS SP5, Leica Microsystems, Wetzlar, Germany) with a 10× objective lens. A benchtop JEOL Neoscope was utilized for all SEM image acquisition at 5 kV or 10 kV. Visualization of cell binding onto scaffolds was conducted via epifluorescent microscopy (Nikon TS 100-F, Nikon Instruments Inc., Melville, USA).

X-ray photoelectron spectroscopy (XPS) was used to investigate the surface chemical composition of the samples before and after oxygen plasma treatment. All XPS spectra were collected using a K-α X-ray photoelectron spectrometer (Thermo Fischer Scientific) using monochromatic X-rays focused to a 400 μm spot size. Excessive sample charging was minimized using a flood gun. Survey spectra were obtained at a pass energy of 100 eV while high resolution peak scans were performed at a 20 eV pass energy. The peak scans were employed to obtain the elemental composition of C, O and N. The C_{1s} binding energies of the samples were accurately established by charge shift correction of the lowest binding energy peak of the C_{1s} to 284.6 eV.

b. Vacuum Plasma Apparatus. A custom built vacuum plasma setup was employed for scaffold treatment. Briefly, a glass chamber housed two fixed electrodes; a grounded electrode located directly below a generator electrode. Plasma was generated at the grounded electrode using a High Voltage RF generator (T&C Power conversion, Inc., USA). The chamber was coupled to a vacuum pump and gas line to enable O_2 gas flow into the chamber.

Methods. *a. Nylon 6,6 3D Fiber Scaffold Fabrication.* Conventional nonwoven manufacturing techniques were used to produce the nonwoven nylon 6,6 scaffolds. In brief, the following process was followed: crimped 15 Denier nylon 6,6, of cross-section diameter 35 μm was processed on a 300 mm wide sample card to form a web. The web was hydro entangled to consolidate the fabric and reduce thickness. The fabric was then hot-pressed at 85 °C for 1 min to achieve the desired thickness (1 mm) without fusing the fibers. This ensured that the scaffolds remained porous and three-dimensional. Samples were cut from the fabric into 14 mm disks and the weight

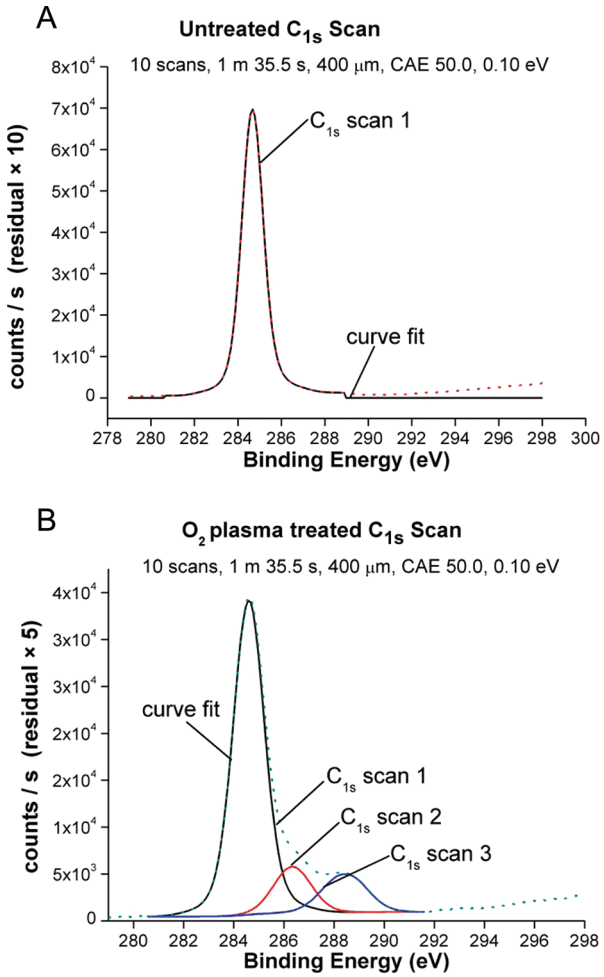

Figure 2. XPS C_{1s} spectra of an O_2 gas plasma treated and untreated 14 mm 2D nylon 6,6 discs. Two new C_{1s} peaks were observed at 286.38 and 288.38 eV for the O_2 plasma-treated sample.

Table 1. Percent Elemental Surface Composition of Treated and Untreated Samples Using XPS

element	at % untreated ± SE	at % O_2 plasma treated ± SE
O	6.78 ± 0.14	22.49 ± 0.45
N	1.63 ± 0.03	1.53 ± 0.03
C	91.60 ± 1.83	75.98 ± 1.52

range utilized was within 1 standard deviation (weight range 0.019–0.024 g).

b. O_2 Plasma Treatment and Silane Functionalization. O_2 Plasma Treatment. 3D scaffolds of fixed dimension were washed in absolute ethanol and water, three times in each solvent and dried under vacuum at 40 °C. After securing the vacuum plasma chamber a complete vacuum was established (P = 2.2–2.7 × 10^1 Pa). The chamber was purged with O_2 ($P = 6 \times 10^2$ Pa) and held under vacuum only ($P = 2.7 \times 10^1$ Pa), each for 1 min and the process was repeated twice. Still under vacuum, O_2 gas was continuously flowed into the chamber and adjusted to 6.3 × 10^1 Pa. O_2 plasma was ignited for 3 min: P = 6.3–6.7 × 10^1 Pa; Forward Power HV = 30 W; Rev Power =17 W. Post treatment, the plasma and vacuum pump were switched off and oxygen was allowed to fill the chamber to ambient pressure. Unless specified, all scaffolds were pretreated with oxygen plasma prior to silanization.

Silane Modification. Immediately after plasma treatment, samples were placed into a clean polypropylene tube containing 50 mL of fresh dehydrated isopropanol combined with 1 mL of (3-mercapto-propyl)-trimethoxysilane, (MPS) or (3-amino-propyl)-trimethoxysilane, (APS) and the lids secured. The scaffolds were allowed to react overnight, washed with fresh isopropanol three times and dried under vacuum at 60 °C. This process led to reproducible silane functionalization of the nylon surface. The silane-functionalized matrices were stored desiccated at room temperature.

Determination of Sulfur Content. The total sulfur content of modified and unmodified scaffolds was assessed by elemental analysis and Ellman's reagent assay. For the elemental analysis, the scaffolds were moistened with phosphoric acid and combusted in a quartz tube in a flow of oxygen at 950 °C. The combustion gases were then passed into a stream of hydrogen at 1200 °C. This converted the sulfur to hydrogen sulphide which was absorbed in a zinc acetate solution. After reacting with ethylene blue, spectrophotometry was used to measure the sulfur content.

For the Ellman's reagent assay, the reaction buffer was prepared as follows: a solution of 0.1 M sodium phosphate dibasic heptahydrate (Fluka, USA) buffer pH 8.0 was combined with 1 mM EDTA. A dose dependent assay was produced by modifying incubating triplicate matrix sets with 0 μL, 5 μL, 50 μL, 250 μL, 500 μL, 1000 or 1500 μL of MPS per 50 mL of 2-propanol, respectively. The scaffolds were then washed in 2-propanol and dried at 40 °C overnight in a vacuum oven. Dried MPS-treated scaffolds were immersed in a mixture of PBS (pH 7.4) and Tris(2-carboxyethyl)phosphine (TCEP) (5 mM final concentration) and allowed to react for 1 h with TCEP to reduce any disulfide bonds. After being extensively rinsed with Ellman's reaction buffer (pH 8), the scaffolds were incubated in 2.75 mL of solution containing Ellman's reagent (0.2 mg). The samples were incubated with the solution under agitation for 15 min. The absorbance at 412 nm of the solutions was measured after removal of the scaffolds using a UV-spectrophotometer at room temperature (Varian Cary 3E). Cysteine monohydrate was used to determine the standard curve. The sulfur content for the samples was then calculated on the basis of the standard curve.

c. Quantum Dot Surface Assembly. The scaffolds were incubated with NC core/shells at a concentration of 10 μM to confirm the presence of primary amine groups. Silane functionalized matrices were combined with NCs (20–60 μL) in 3–5 mL of 2-propanol and mixed on a motorized wheel at minimum speed for 1 h. Following incubation, the matrices were washed in three volumes of fresh 2-propanol and then dried at room temperature under argon. A portable UV light box was utilized to confirm the deposition of NCs. The NC-coated matrices were then observed in more detail under confocal microscopy using the 514 nm line of an argon ion laser and at a magnification of 100× and 200×.

d. Protein Functionalization. Dried MPS-treated scaffolds were immersed in a mixture of PBS (pH 7.4) and Tris(2-carboxyethyl)-phosphine (TCEP) (5 mM final concentration) and allowed to react for 1 h with TCEP to reduce any disulfide bonds. After 1 h, between 50 μL–1 mL of 1 mg/mL mNtv dissolved in PBS (pH 7.4) was combined with the scaffold and the total volume increased to 30 mL with fresh PBS. The scaffolds were allowed to react overnight. The mNtv-functionalized scaffolds were then washed in PBS (pH 7.4) several times and transferred to fresh PBS (pH 7.4) for storage at 4 °C.

e. Enzyme-Linked Immunosorbent Assay (ELISA). All samples were analyzed in triplicates. Scaffolds were blocked in a 96-well cell culture plate in 5% w/v skim milk solution (dissolved in PBS, pH 7.4) for 3 h. Blocked scaffolds were washed three times in 0.05% w/v PBS/Tween 20 solution (PBST). Each scaffold was then incubated with biotin-HRP at a 1:1000 dilution for 20 min on an orbital shaker at 80 rpm. This was followed by three washes in 100 μL PBST, then 100 μL of fresh PBS and Substrate Reagent Kit was added to all scaffolds. The scaffolds were incubated for 20 min in the dark on an orbital shaker for 20 min. Sulfuric Acid (1M) was administered to all scaffold containing wells to stop the colorimetric reaction. Finally, 100 μL from all test wells were transferred to a new plate and the absorbance read at λ = 450 nm on a TECAN GENios Pro Microplate Reader.

f. Cell Selection Using mNtv-functionalized Nylon Scaffolds. The ability for mNtv-functionalized scaffolds to specifically select for a

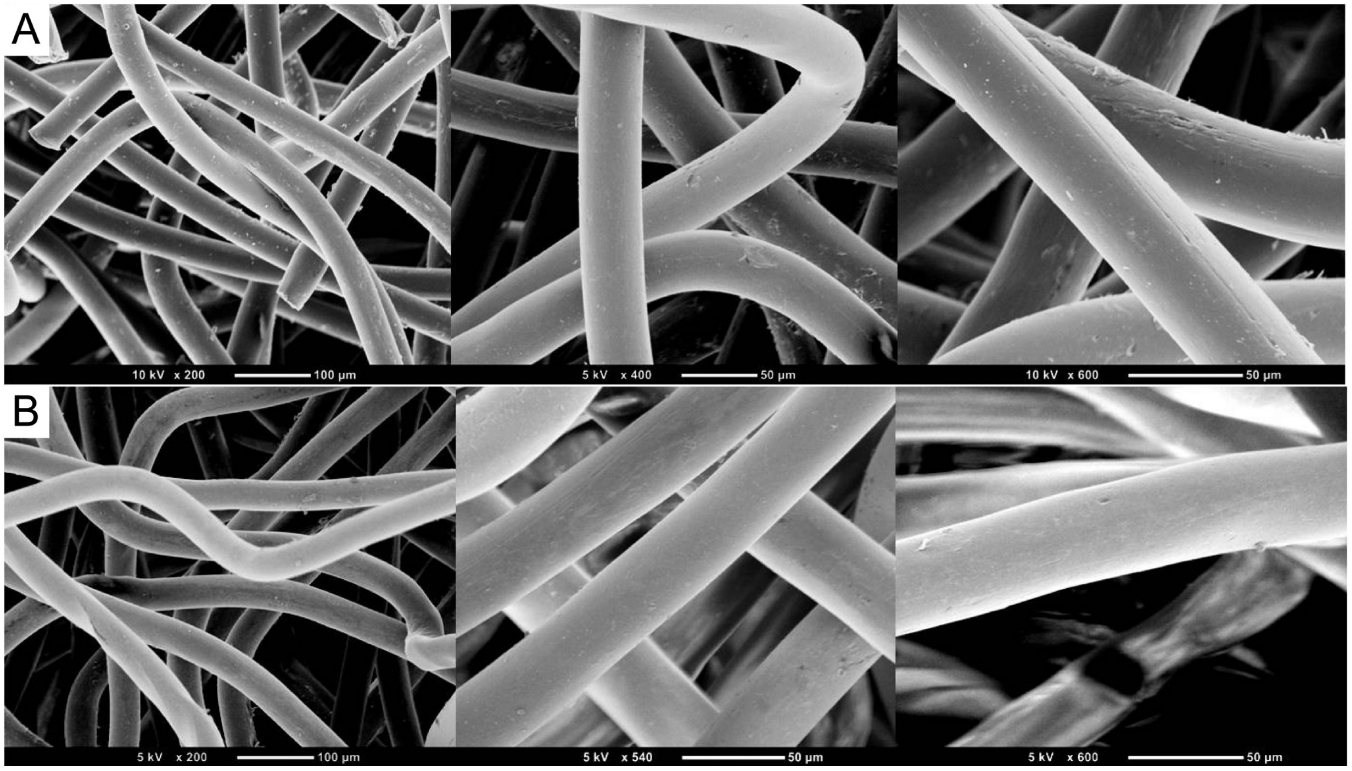

Figure 3. SEM analysis of nylon scaffold silane modification procedure. (A) Unmodified, (B) silane modified. The silanization process did not alter the scaffold surface topography.

particular type of cell was assessed using CD3 T cells. CD3 T cells are a group of white blood cells and within this population, there are two subgroups, CD4 and CD8 cells. The mNtv-scaffolds were used to specifically select for CD4 cells within the CD3 population.

Nylon scaffolds that were grafted with mNtv were incubated with either biotinylated CD4 antibody or IgG antibody as a negative control, on a rocker at 37 °C for 15 min. The antibodies were used at a dilution of 1:100 in PBS. The antibody-treated scaffolds were then seeded with 5×10^5 CD3 T cells per scaffold and incubated at 37 °C for 15 min on a rocker. Scaffolds were washed with PBS 3 times and cells attached onto the scaffolds were visualized using LIVE/DEAD Kits for Mammalian Cells, which stains live cells green and dead cells red.

3. RESULTS

Each unmodified nylon 6,6 fiber scaffold first underwent surface modification to enable silane attachment. To achieve this, we exposed scaffolds to O_2 gas plasma. XPS was employed to identify oxygen species introduced to the native surface post O_2 plasma treatment. When XPS was conducted on 3D nylon 6,6 scaffolds, it was discovered that accurate spectrum fitting could not be achieved due to the material's geometry. The high porosity of the scaffold generated large background signals caused by electron scattering. Therefore, XPS was carried out on 2D nylon 6,6 disk to demonstrate the effect of O_2 plasma treatment on nylon. Relative to an untreated sample of 14 mm 2D nylon 6,6 disk (Figure 2A), the XPS response patterns in the C_{1s} region (Figure 2B) collected from a plasma treated sample identified the emergence of two additional peaks at 286.38 and 288.38 eV, respectively. Peaks detected at these binding energy positions corresponded to the formation of functional oxygen groups C−O, C═O and O═C−O.[36] As shown in Table 1, there was more oxygen species in the O_2 plasma-treated samples (22.49%) when compared to untreated samples (6.78%), demonstrating the typical effects of polymer exposure to O_2 gas plasma.[25,26]

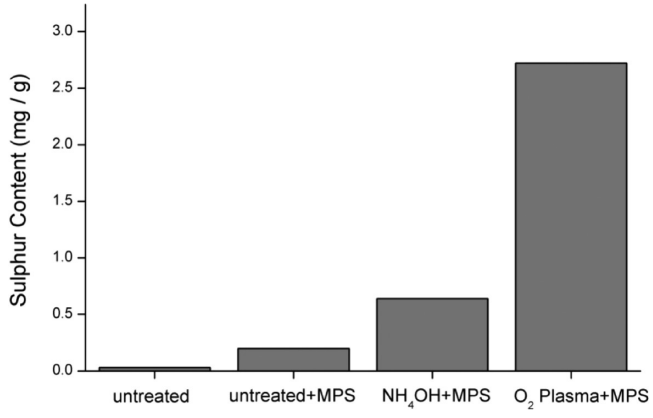

Figure 4. Sulfur content analyzed by elemental analysis. Results acquired for various treated scaffolds exhibited the highest sulfur content in the oxygen plasma-treated group.

Following plasma treatment matrices were immediately reacted with mercapto- or amino-functional silane (MPS or APS) dissolved in 2-propanol at room temperature. A series of surface characterization and validation studies of the silane modified scaffolds were conducted, including examination of: surface topography, silane attachment efficiency to assess the benefit of O_2 plasma pretreatment, surface chemical characterization (Elemental analysis, Ellman's reagent assay, surface reporting using fluorescent quantum dots) and the potential for the scaffolds to be bioconjugated.

It is important that post silanization, the surface topography of the scaffold mimics that of the native material. Scanning

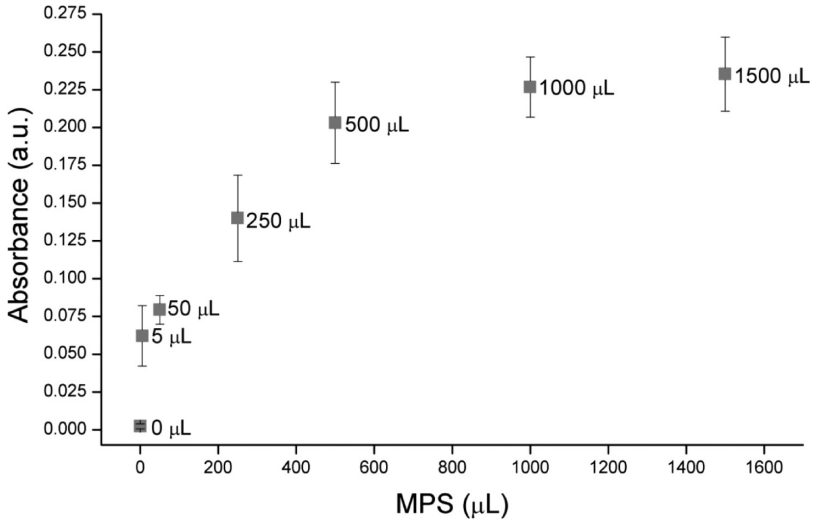

Figure 5. Sulphydryl surface characterization assay. Ellman's reagent was employed to quantitate the concentration of surface bound sulphydryl groups on single O_2 plasma-treated, MPS-modified scaffolds.

electron microscopy was used to investigate the scaffold surface pre and post silane modification. The 3D fibrous (35 μm cross-section diameter) network is clearly identified in panels A and B (Figure 3). No differences were observed in the fiber dimensions, network morphology of the scaffold and porosity between the two samples. Furthermore, silane modification did not significantly alter the surface topography of the fibers. Nevertheless, high-resolution SEM could not confirm the presence of silane on the polyamide surface; hence, a quantitative chemical analysis of the scaffold post silanization was carried out.

The presence of sulfur in modified and unmodified nylon was measured as sulfur is an elemental marker related to the presence of MPS (-SH). The efficacy of the silanization procedure was also assessed. A sample set was pretreated with 8% (v/v) ammonium hydroxide (NH_4OH+MPS) solution in order to hydrolyze the surface[37,38] and to provide an alternative comparison for the presilane plasma-activation step. Individual scaffolds (14 mm disks weight range 0.019−0.024 g) were analyzed for total sulfur content (pre and post silanization); tests groups included: (i) untreated + MPS, (ii) NH_4OH + MPS, (iii) O_2 plasma + MPS, (iv) untreated scaffold (Figure 4). Analyzed in triplicates, the results from the elemental analysis revealed increased presence of sulfur in MPS-treated samples. Additionally, O_2 plasma treatment showed an increase in MPS content of 4 and 13-fold when compared to NH_4OH + MPS-treated and unmodified scaffolds, respectively. These data complemented the XPS results, confirming the increase in % sulfur composition (MPS) after O_2 plasma treatment. On the basis of this outcome, all scaffolds were pre-exposed with O_2 plasma prior to silanization.

The elemental analysis provided a quantitative, yet destructive approach to detect total sulfur content for individual MPS modified scaffolds. Therefore, a nondestructive technique was employed to detect and quantitate surface-bound thiols on the MPS modified scaffold (14 mm diameter disk) using an Ellman's reagent assay (Figure 5). As a function of MPS volume used in the modification procedure, the plateau phase started at 500 μL ($\cong$ 0.78 mM). The method we selected to modify the scaffolds for bioconjugation utilized a 1 mL of MPS (in 50 mL of 2-propanol) which equated to a 0.94 mM (absorbance 0.23) concentration of surface bound -SH detected on the single MPS modified (0.023 g) scaffold. The volume of MPS utilized (1 mL) produces scaffolds with surface bound thiol concentrations well within the plateau region of the dose-dependent plot.

Characterizing the surface chemistry of a 3D scaffold using nondestructive analytical methods presents a far greater challenge compared to a 2D polymeric film. Recently, CdSe/ZnS NCs stabilized in aminopentanol were shown to specifically attach to an $-NH_2$-modified surface.[39] Utilizing this knowledge, the present study employed fluorescent semiconductors to operate as NH_2 reporters for an APS-modified 3D scaffold. Confocal microscopy images are presented in Figure 6. The results showed the absence and presence of NCs (λ_{max} = 572 nm) after incubation with an unmodified (control panel A) and APS-modified scaffold (Figure 6B, C), respectively. Negligible fluorescence was detected from the unmodified scaffold. Comparatively high levels of fluorescence were detected throughout the APS-modified 3D scaffold. It was observed that this surface reporting technique did not require high precision microimaging and can be conducted using a conventional benchtop UV light.

The ability to functionalize the silane-modified 3D scaffold with biomolecules was also investigated using a standardized bioconjugation protocol. The biomolecule employed for scaffold functionalization is a neutravidin protein which has been modified with a maleimide linker designed specifically to interact with thiol species. Maleimide neutravidin (mNtv) also has greater affinity to biotinylated molecules compared with streptavidin. Further to functionalization of the silane modified scaffold, the binding stability of mNtv to the scaffold was ascertained by comparing the levels of mNtv on unmodified scaffold (nonspecifically adsorbed) to MPS modified scaffold over a period of time using ELISA (Figure 7). Triplicate samples were incubated in either 70% EtOH at 4 °C or PBS pH 7.4 at RT for 4 months. Protein levels detected from MPS modified scaffolds were 58% (PBS) and 45% (EtOH) higher, respectively, compared to mNtv that was adsorbed onto unmodified scaffolds. The relative absorbance profiles measured between test groups were consistent throughout the storage period.

The mNtv-functionalized scaffolds were used to specifically select CD4 cells, a subgroup from CD3 cells. As shown in

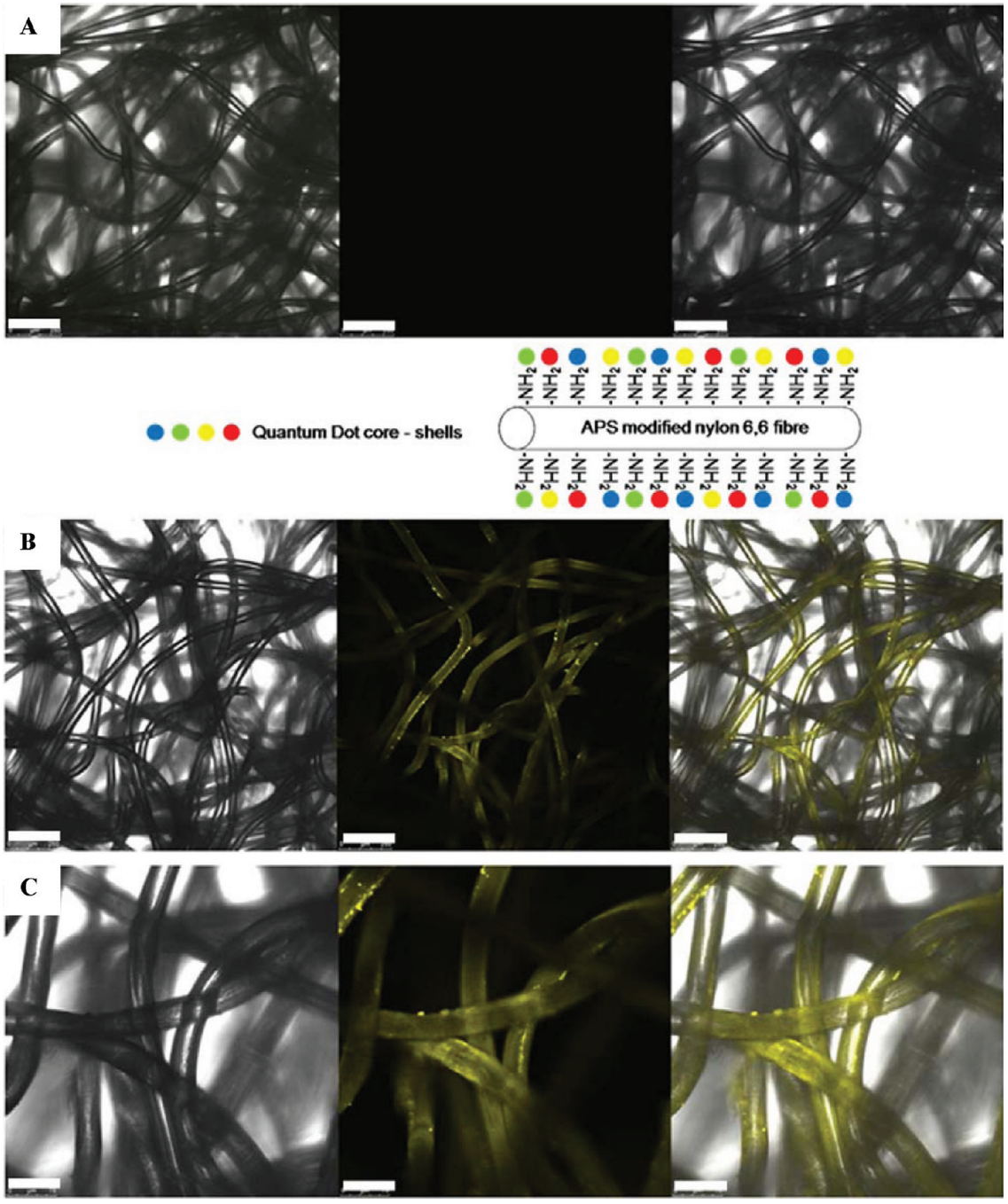

Figure 6. CdSe/ZnS nanocrystal (NC) Surface Reporters. Image sequence captured with a 10X (A and B) and 20X (C) objective. From left: transmission, fluorescence, and two-channel overlay. (A) Unmodified scaffold + NC. (B) APS-modified scaffold + NC. (C) A higher magnification (200×) of the APS -modified scaffold + NC showing the NC fluorescence emission being observed throughout the silane modified scaffold. The scale bars denote 250 μm for A and B, and 75 μm for C.

Figure 8, scaffolds that were incubated with antibody specific to CD4 exhibited cell binding (D−F). Cells seeded onto scaffolds that were incubated with the nonspecific antibody, IgG, were not bound to the fibers. Most of the cells were observed at the bottom of the well, with some cells floating within the scaffolds.

4. DISCUSSION

The objective of this investigation was to develop a simplified silane-based technique to biofunctionalize 3D nylon 6,6 scaffolds. To address the aforementioned research objectives, we presented the following outcomes:

1. Develop a Two-Step Surface Modification Involving Plasma and Silane Chemistries for a 3D Nylon 6,6 Porous Scaffold. A simple robust silanization method for nonwoven nylon 6,6 fiber scaffolds was developed. The procedure does not rely solely on composite technology, gas phase surface modification and does not have multiple procedural steps. The modification approach combines O_2 gas plasma treatment and a wet chemical silane-based functionalization which enables routine direct silane modification of the scaffold system. The method does not alter the scaffold's surface topography or pore network; it maintains the native 3D architecture

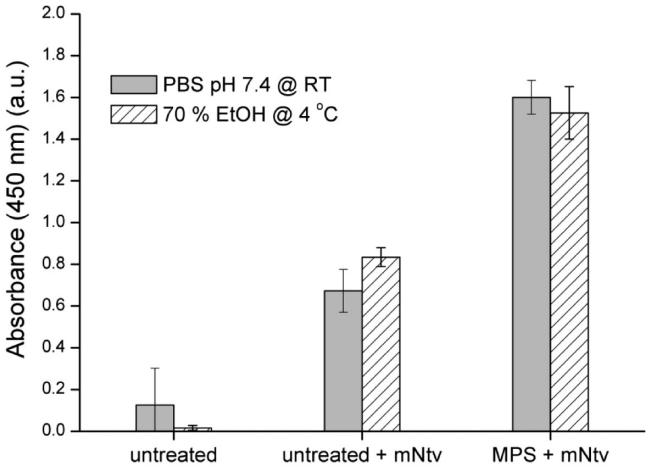

Figure 7. Stability of maleimide neutravidin-functionalized scaffold. Three scaffolds sets were tested: untreated scaffold (control), unmodified scaffold functionalized with maleimide neutravidin (mNtv) (control), and (3-mercaptopropyl)trimethoxysilane (MPS)-modified scaffold functionalized with mNtv. Triplicate sets were stored in PBS pH 7.4 at room temperature (RT) and 70% EtOH at 4 °C. After 4 months, the protein levels were probed using a biotinylated horse radish peroxidase (biotin HRP) enzyme. The silanized scaffold provided a more chemically robust platform for thiol-specific binding proteins.

and, moreover, generates a bioactive surface-anchoring system. The two-step approach is amenable to nylon 6,6 of various geometries and various other polymers with a low affinity to direct silane functionalization.

2. Validate the Presence of MPS (−SH) and APS ($-NH_2$) Silane on a Modified Scaffold. Elemental analysis was initially used to confirm the presence of MPS (total sulfur content) on single 3D scaffolds of fixed dimension post silane modification. Results revealed a pretreatment step with O_2 gas plasma produced scaffolds with the highest silane coupling efficiency (2.72 mg/g). A non destructive approach was then employed to quantitate the concentration of surface bound sulphydryl groups on single O_2 plasma treated MPS modified scaffolds. For 1 mL of MPS used, Ellman's reagent detected a 0.94 mM concentration of MPS (−SH) on the 14 mm diameter scaffold surface. The volume of MPS used corresponded to a final concentration well within the plateau range of a volume-dependent analysis and midrange of the cysteine hydrochloride monohydrate standard curve fit.

Surface characterization of two-dimensional substrates can be completed with ease. However, the 3D scaffold presented a challenge using standardized 2D characterization tools. To overcome the obstacle, we developed a rapid fluorescence surface reporting tool using CdSe/ZnS quantum dot core−shells. The technique is an effective surface characterization approach for APS ($-NH_2$)-functionalized scaffolds.

3. Assess the Ability to Functionalize the Silane-Modified Scaffold with Biomolecules. ELISA analysis confirmed a mercapto-silane-modified scaffold provided a chemically more robust surface for thiol-specific mNtv protein conjugation. This result indicated that the protein layer is more stable when covalently bonded to the scaffold surface as compared to passive adsorption. Furthermore, the functionality of the mNtv-grafted nylon scaffolds was demonstrated by their ability to select for CD4 cells via the use of CD4-specific antibody.

In addition to targeted cell selection, the mNtv-functionalized scaffold has the potential to be utilized in other applications such as enhancement of cell proliferation, tissue engineering and drug delivery. This is because, aside from antibodies, the scaffold system can be conjugated with various types of biotinylated molecules such as growth factors, adhesion ligands and enzymes tailored specifically to the application of interest. While nylon was used as the base polymer, the surface

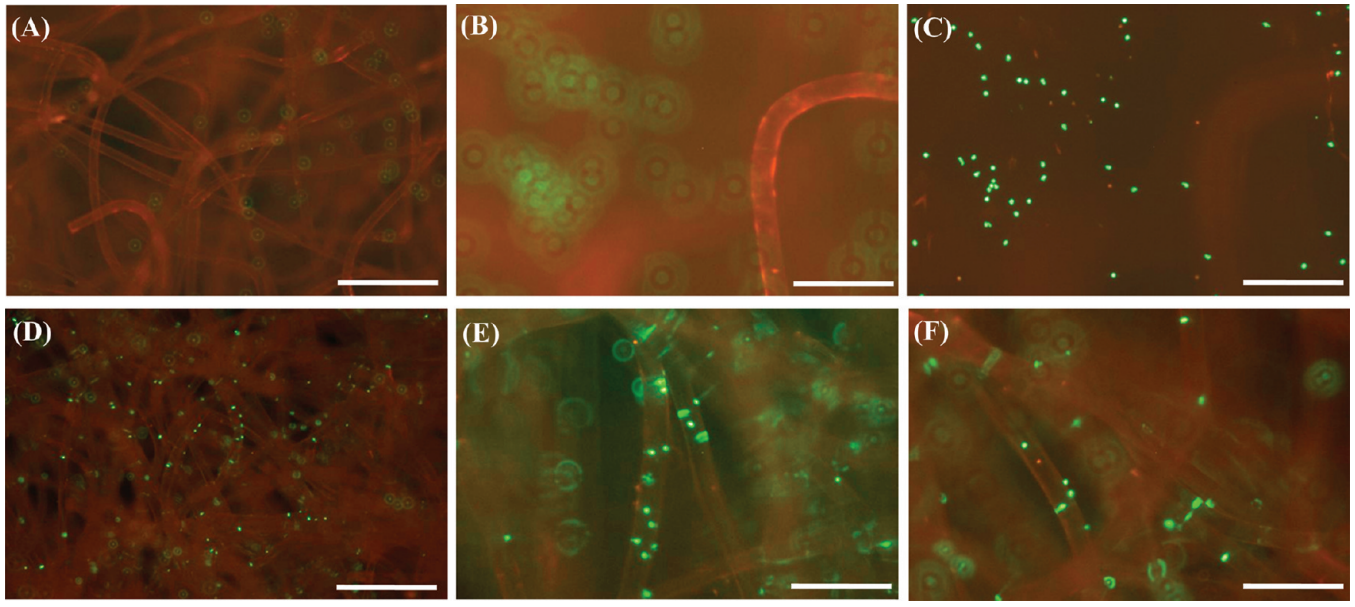

Figure 8. Epifluorescence images of CD4 cells on biofunctionalized scaffolds (40× and 100× magnification). Cells were stained green and the nylon fibers were red. Scaffolds were incubated with either (A−C) biotinylated IgG antibody (negative control) or (D−F) biotinylated antihuman CD4. CD4 cells can be seen attached onto fibers (D) at 40× and (E, F) at 100×, focusing on one focal plane of the fibers, whereas cells in the IgG group were mainly observed (C) at the bottom of the well. No cells were attached on the fibres (A and B, focusing on one fiber). The scale bars denote 500 μm at 40× (A and D) and 100 μm at 100× (B, C, E, and F).

modification technique described in this study can be extended to a variety of polymers, including biodegradable ones, should the scaffolds be used for tissue engineering purposes.

5. CONCLUSION

A two-step silane surface modification approach that enables direct biofunctionalization of 3D nylon 6,6 fiber scaffolds is described in this paper. Using O_2 plasma technology and a silane wet-chemical technique, the conjugation of biomolecules to nonwoven scaffolds fabricated from commercial grade nylon 6,6 fiber can be customized on demand. A potential application of the neutravidin-functionalized scaffold was demonstrated by the specific binding of CD4 cells to the scaffolds. The biocompatible 3D scaffold produced presents a flexible system that may be used as a cell therapy device for targeted cell selection.

AUTHOR INFORMATION

Corresponding Author

* E-mail: xungai.wang@deakin.edu.au. Phone: +61 3 52272894.

Author Contributions

†These authors contributed equally

Notes

The authors declare no competing financial interest.

ACKNOWLEDGMENTS

The kind donation of CdSe/ZnS core/shell nanocrystals from Dr Tich-Lam Nguyen and Christian Potzner of the University of Melbourne, Australia. The authors thank Dr Xiujuan Jane Dai for her X-ray photoelectron spectroscopy measurements and data analysis, as well as her valuable suggestion and discussion. The access to the XPS facility at RMIT University is also acknowledged. Thank you to Mr Graeme Keating for manufacturing the nonwoven nylon scaffolds. Elemental analysis was conducted by CMAS Chemical & MicroAnalytical Services Pty Ltd, Belmont, Australia.

REFERENCES

(1) Hutmacher, D. W. *Biomaterials* **2000**, *21*, 2529.
(2) Xu, S. L.; Li, D. C.; Lu, B. H.; Tang, Y. P.; Wang, C. F.; Wang, Z. *Rapid Prototyping J.* **2007**, *13*, 99.
(3) MacNeil, S. *Nature* **2007**, *445*, 874.
(4) Petrini, P.; Parolari, C.; Tanzi, M. C. *J. Mater. Sci. Mater. Med.* **2001**, *12*, 849.
(5) Elema, H.; de Groot, J. H.; Nijenhuis, A. J.; Pennings, A. J.; Veth, R. P. H.; Klompmaker, J.; Jansen, H. W. B. *Colloid Polym. Sci.* **1990**, *268*, 1082.
(6) Freed, L. E.; Vunjak-Novakovic, G.; Langer, R. *J. Cell. Biochem.* **1993**, *51*, 257.
(7) Chua, K. N.; Chai, C.; Lee, P. C.; Ramakrishna, S.; Leong, K. W.; Mao, H. Q. *Exp. Hematol.* **2007**, *35*, 771.
(8) Li, Y.; Ma, T.; Kniss, D. A.; Yang, S. T.; Lasky, L. C. *J. Hematother. Stem Cell Res.* **2001**, *10*, 355.
(9) Rocha, V.; Gluckman, E. *Br. J. Hamaetol.* **2009**, *147*, 262.
(10) Schoemans, H.; Theunissen, K.; Maertens, J.; Boogaerts, M.; Verfaillie, C.; Wagner, J. *Bone Marrow Transplant.* **2006**, *38*, 83.
(11) Herrera-Alonso, M.; McCarthy, T. J.; Jia, X. Q. *Langmuir* **2006**, *22*, 1646.
(12) Silva, C.; Cavaco-Paulo, A. *Biocatal. Biotransform.* **2008**, *26*, 350.
(13) Kuo, S. M.; Tsai, S. W.; Huang, L. H.; Wang, Y. J. *Artif. Cells Blood Substit. Biotechnol.* **1997**, *25*, 551.
(14) Bezuidenhout, D.; Davies, N.; Black, M.; Schmidt, C.; Oosthuysen, A.; Zilla, P. *J. Biomater. Appl.* **2010**, *24*, 401.
(15) Moroni, L.; de Wijn, J. R.; van Blitterswijk, C. A. *J. Biomater. Sci., Polym. Ed.* **2008**, *19*, 543.
(16) Howarter, J. A.; Youngblood, J. P. *Macromolecules* **2007**, *40*, 1128.
(17) Jiao, Y.-P.; Cui, F.-Z. *Biomed. Mater.* **2007**, *2*, R24.
(18) Ikada, Y. *Biomaterials* **1994**, *15*, 725.
(19) Li, Y.; Yu, J.; Guo, Z. X. *J. Appl. Polym. Sci.* **2002**, *84*, 827.
(20) Shim, J. H.; Choi, J. H.; Joo, J. H.; Yoon, J. S. *Key Eng. Mater.* **2007**, *334*−*335*, 877.
(21) Orendorff, C. J.; Huber, D. L.; Bunker, B. C. *J. Phys. Chem. C* **2009**, *113*, 13723.
(22) Shearer, A. E. H.; Paik, J. S.; Hoover, D. G.; Haynie, S. L.; Kelley, M. J. *Biotechnol. Bioeng.* **2000**, *67*, 141.
(23) Siow, K. S.; Britcher, L.; Kumar, S.; Griesser, H. J. *Plasma Process. Polym.* **2006**, *3*, 392.
(24) Dai, X. J.; Plessis, J. d.; Kyratzis, I. L.; Maurdev, G.; Huson, M. G.; Coombs, C. *Plasma Process. Polym.* **2009**, *6*, 490.
(25) Dai, X. J.; Elms, F. M.; George, G. A. *J. Appl. Polym. Sci.* **2001**, *80*, 1461.
(26) Murakami, T.; Kuroda, S.-i.; Osawa, Z. *J. Colloid Interface Sci.* **1998**, *202*, 37.
(27) Tsougeni, K.; Vourdas, N.; Tserepi, A.; Gogolides, E.; Cardinaud, C. *Langmuir* **2009**, *25*, 11748.
(28) Charles, C.; Boswell, R. W. *J. Appl. Phys.* **1998**, *84*, 350.
(29) Moon, S. I.; Jang, J. *J. Adhes. Sci. Technol.* **2000**, *14*, 493.
(30) Yamada, M.; Amoo, M. *Int. J. Biol. Macromol.* **2008**, *42*, 478.
(31) Saini, G.; Sautter, K.; Hild, F. E.; Pauley, J.; Linford, M. R. *J. Vac. Sci. Technol., A* **2008**, *26*, 1224.
(32) Nuhiji, E.; Mulvaney, P. *Small* **2007**, *3*, 1408.
(33) Nuhiji, E.; Mulvaney, P.; Poetter, K. International Patent Application PCT/AU2009/001515, 2009; p 103.
(34) van Embden, J.; Mulvaney, P. *Langmuir* **2005**, *21*, 10226.
(35) Jasieniak, J.; Mulvaney, P. *J. Am. Chem. Soc.* **2007**, *129*, 2841.
(36) Cui, S.; Shen, X.; Lin, B.; Jiang, G.; Zhang, W. *J. Wuhan. Univ. Technol.* **2008**, *23*, 436.
(37) Elmore, J. D.; Goff, E. S. Celanese Corporation: New York, 1987.
(38) Lee-Sullivan, P.; Chian, K. S.; Yue, C. Y.; Looi, H. C. *J. Mater. Sci. Lett.* **1994**, *13*, 305.
(39) Gomez, D. E.; Pastoriza-Santos, I.; Mulvaney, P. *Small* **2005**, *1*, 238.